AIAA 80-1330R

Combination of Kinematics with Flow Visualization to Compute Total Circulation

James G. Brasseur*
NASA Ames Research Center, Moffet Field, Calif.
and
I-Dee Chang†
Stanford University, Stanford, Calif.

A method is described in which kinematics is exploited to compute the total circulation of a vortex from relatively simple flow visualization experiments. There are several advantages in the technique, including the newly acquired ability to calculate the changes in strength of a single vortex as it evolves. The main concepts and methodology are discussed in a general way for application to vortices which carry along with them definable regions of essentially irrotational fluid; however, the approach might be generalized to other flows which contain regions of concentrated vorticity. As an illustrative example, an application to the study of the transient changes in total circulation of individual vortex rings as they travel up a tube is described, taking into account the effect of the tube boundary. The accuracy of the method, assessed in part by a direct comparison with a laser Doppler measurement is felt to be well within experimental precision for vortex rings over a wide range of Reynolds numbers.

Introduction

FLOWS with regions of concentrated vorticity are commonly found in nature at all scales and play a fundamental role in countless problems of both practical and academic interest.[1] The evolution of a vortex can be described in large part by the changes in total circulation, or strength as a function of time. These changes involve complicated dynamic processes of vorticity diffusion and convection from the regions where vorticity is concentrated, the instabilities and breakdown mechanisms of the vortex, the development of small scales of turbulence which enhance diffusion, and so on. It would be of considerable interest, therefore, to be able to measure the transient changes in total circulation for different vortex systems as they evolve—initially, perhaps, for isolated vortices, but eventually for more complicated vortex systems involving several interacting vortex elements.

A measurement of circulation at even one point in time, however, is difficult to obtain. In the past these measurements have required a knowledge of the velocity field within the vortex. To measure the total circulation of vortex rings, for example, the velocity around the vortex core has been measured using laser Doppler velocimeters (LDV)[2,3] and hot-wire[4] anemometers, then integrated to find the circulation. Such an approach, however, requires a repeatable production of vortices, precluding the possibility of calculating the strength of a single vortex as it evolves.

We introduce in this paper a technique for computing the total circulation of a vortex in an incompressible flow by combining relatively simple flow visualization measurements with relationships derived from the kinematic properties of the vortical flowfield. With this approach total circulation is computed for an individual vortex at any point in its evolution, so the method can be applied to study the dynamic changes in strength of individual vortices as they evolve in time. Furthermore, flow visualization generally involves considerably less expense than laser Doppler systems, and there is no concern with flow interference as there is with hot-wire measurements.

The method as described here applies to what we call "closed" vortex systems—a vortex or system of vortices where well-defined regions of essentially irrotational fluid are carried along with the vortex cores. Two basic examples are the vortex pair and the vortex ring. We might also expect that this approach could be generalized and applied to other flows in which are embedded regions of concentrated vorticity.

The method has been developed and applied in an extensive study of the transient changes in total circulation of vortex rings as they are formed and as they evolve, for vortex rings from very low to very high Reynolds numbers. For the purposes of this discussion, however, the vortex ring development will serve as an example to illustrate an application of the method and will necessarily be brief. The details of the mathematical development and a complete discussion of the results of this study can be found in Ref. 5 and will be forthcoming in future publications.

Preliminary Concepts

Kinematics of a Vorticity Field

Consider an incompressible flow where at time t the velocity at point x is given by $u(x)$ and the vorticity at point ζ by $\omega(\zeta)$. Thus we have

$$\nabla \cdot u = 0 \tag{1}$$

$$\nabla \times u = \omega \tag{2}$$

Using only these two expressions one can derive the well-known law of Biot and Savart,[6] which for a bounded flow is

$$u(x) = -\frac{1}{4\pi} \iiint_{\text{flowfield}} \frac{r \times \omega(\zeta)}{r^3} \, d\zeta^3 + u_i(x) \tag{3}$$

where $r = x - \zeta$ and $r = |r|$. u_i is an irrotational and solenoidal velocity chosen to satisfy the boundary conditions. Two important properties of this equation should be given special note. First, Eq. (3) is a purely kinematic expression

Presented as Paper 80-1330 at the AIAA 13th Fluid and Plasma Dynamics Conference, Snowmass, Colo., July 14-16, 1980; submitted Sept. 18, 1980; revision received Feb. 19, 1981.

*NRC Research Associate; currently, Research Fellow, Dept. of Aeronautics and Astronautics, University of Southampton, England. Member AIAA.

†Professor, Dept. of Aeronautics and Astronautics. Member AIAA.

since only conservation of mass is used in its derivation. Thus, even for a time-dependent flow, laminar or turbulent, where vorticity is being diffused and convected, if at any given time the vorticity field is known or can be well approximated, the velocity field can, in principle, be computed from Eq. (3). Second, since the velocity is related linearly to the vorticity, the vorticity field can be divided into elements and the velocity field for each individual element summed to find the total velocity field.

By considering together with Eq. (3) the kinematic expression which relates the total fluid impulse to an integral over the vorticity field[6] one can think of the vorticity field as an impulsively created source field which at each point in time "induces" the velocity field. Dynamic processes, as described by the vorticity equation, control the evolution of this source field (that is, the changes in distribution and strength of the sources); however, from a knowledge of the source field, the velocity field can be kinematically constructed through the Biot-Savart law. In other words, whereas dynamics controls the evolution of the vortical flowfield, the role of kinematics is to relate this vorticity field at every instant in time to the velocity field.

Kinematics of a Vortex

In a vortex flow vorticity is concentrated along a curved line in a region called the vortex core; the total circulation, or strength of the vortex, is the integral of vorticity through the core cross section. In general, lesser amounts of vorticity reside outside the vortex core; however, depending to a large extent on Reynolds number, the vorticity is often sufficiently concentrated that an accurate approximation can be obtained by confining the total circulation to a vortex tube and neglecting the effects of residual vorticity elsewhere.

For mathematical simplicity it would be advantageous to idealize this vortex tube as a single vortex filament. The accuracy of such an idealization, however, depends on the extent to which vorticity is concentrated and on the region of the flow in which we are interested. Let us describe the degree of concentration of vorticity in the core by the ratio a/R where a is some effective core radius and R the local radius of curvature. If a/R is sufficiently small, then, the irrotational velocity field in a region sufficiently far from the vortex core should be accurately described by shrinking the core to a filament of the same strength (the flow in the core must, of course, take into account the details of the vorticity distribution). In fact, for a perfectly two-dimensional vortex ($R\to\infty$), this idealization is exact.

In the irrotational region away from the vortex core, the velocity can be represented by a velocity potential Φ defined by

$$u=\nabla\Phi \tag{4}$$

The potential for a vortex filament loop of strength Γ can be derived from Eq. (3)

$$\Phi(x)=\int\int_A \frac{\partial}{\partial n}\left(\frac{\Gamma}{4\pi r}\right)dA(\zeta)+\Phi_i(x) \tag{5}$$

where A is a surface bounded by the loop, n is the outward normal to that surface, and $r=x-\zeta$; Φ_i is the potential field induced by the presence of boundaries and must satisfy Laplace's equation. From Eq. (5) we see that away from the vortex core the potential field, and therefore the streamline and velocity fields of a vortex, is kinematically described by its strength and its geometrical orientation in the flowfield.

Combining Kinematics with Flow Visualization

Basic Method

The goal is to devise a measurement technique whereby the strength of a vortex can be computed from relatively simple flow visualization experiments. We have found in considering Eq. (3) that the velocity field is kinematically related to the vorticity field at each instant in time. Furthermore, if the vorticity is sufficiently concentrated, the vortex core can be modeled as a filament and the flowfield away from the core calculated from the much simpler integrations of Eq. (5). Thus, there exists a kinematic relationship between the potential field and the strength and geometrical orientation of the vortex. Let us represent this functional relationship symbolically as follows:

$$\Phi=\Phi(\Gamma,\text{geometry}) \tag{6}$$

In a flow with more than one vortex element the potential would be obtained by summing over the potential fields of the individual elements.

Equation (6) represents kinematic relationships between the potential field and quantities describing the vortex, relationships which must be satisfied at each instant in time. However, we could just as well have written these relationships in the inverted form

$$\Gamma=\Gamma(\Phi,\text{geometry}) \tag{7}$$

That is, from a knowledge of the potential field and the geometry of the vortex, we can, in principle, calculate the total circulation. It is this missing knowledge needed to compute Γ which is obtained from flow visualization experiments.

To relate the total circulation and geometry of a vortex to its potential field, we model the core as a filament of strength Γ (the accuracy of such a model will depend on the degree to which the vorticity is concentrated and should ultimately be tested). Then, using Eq. (5) we compute relationships between the total circulation and parameters which describe both the potential field and the geometry of the vortex. These relationships, symbolically expressed by Eq. (7), are purely kinematic in nature and apply at each instant in time (to the accuracy of the model). From flow visualization experiments, then, we measure the parameters which describe the potential field and geometry, insert this information into the previously computed kinematic relationships, and calculate the total circulation, Γ.

Experimentally we can follow the development of a vortex and measure the needed parameters as a function of time, thus allowing for a dynamic calculation of the transient changes in total circulation for an individual vortex as it evolves. It should be kept in mind, however, that the dynamics enters through the experimental measurements; the role of kinematics is to relate these measured parameters at all times to the total circulation of the vortex.

Kinematic Relationships for a Closed Vortex

It is not clear at this point which parameters describe the potential field and how they are to be computed. The answer is to some extent problem-dependent. We consider here a closed vortex (or closed-vortex system), which, as mentioned in the Introduction, is a vortex which carries along with it a definable region of essentially irrotational fluid. We shall call this region of irrotational fluid the "bubble." The extent of the bubble will depend on the strength and geometry of the vortex and on the velocity with which it is convected through the flow. We find that from the size and shape of the bubble and the velocity of the vortex system, we can derive the needed parameters which are to be related kinematically to the total circulation of the vortex.

Examples of closed vortices are the vortex ring and the vortex pair. Vortex rings, as shown schematically in Fig. 1, consist of a toroidal core region where vorticity is concentrated, an outer spheroidal bubble which is confined and transported along with the core, and a wake region which results from the diffusion of vorticity from the vortex core and convection out of the vortex ring. LDV measurements by

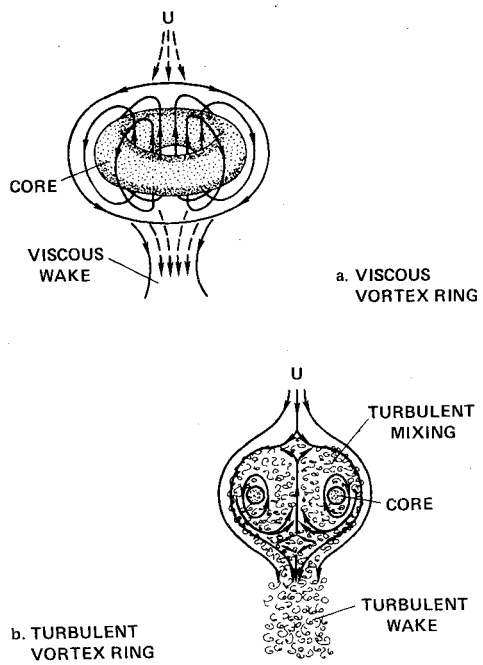

Fig. 1 The structure of vortex rings in a frame fixed to the moving vortex.

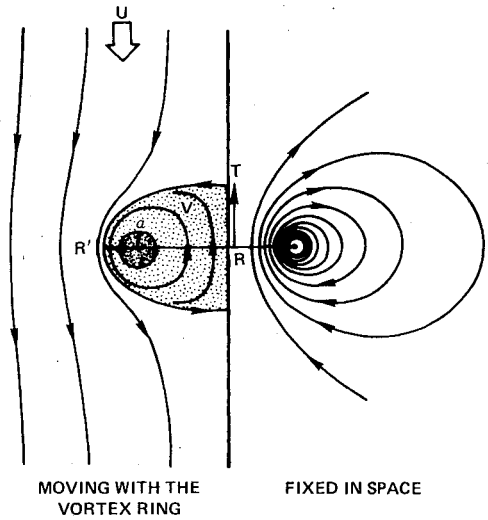

Fig. 2 The streamlines of a vortex ring in moving and fixed frames of reference.

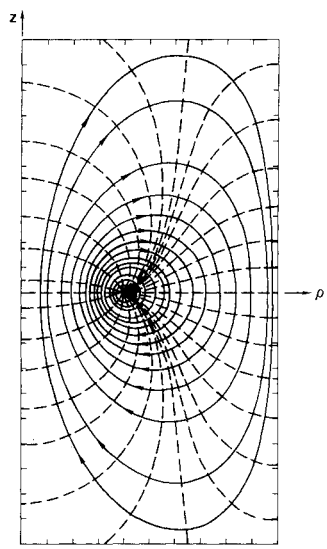

Fig. 3 Streamlines and lines of constant potential in the fixed frame for a bounded vortex ring, $\epsilon = 0.40$.

Maxworthy[2] and Sullivan et al.[3] show that the vorticity is highly peaked in the core, with smaller amounts out to the edge of the bubble. Vortex rings at higher Reynolds numbers tend to have more compact cores than those at lower Reynolds numbers. The LDV measurements, for example, indicate that $a/R \sim 0.10 \rightarrow 0.15$ for $Re \sim 20{,}000$, but at $Re = 3040$ $a/R \sim 0.27$, where $Re = 2RU/\nu$. The loss of vorticity to a wake results in a decrease in strength and impulse of the vortex in time.

As an illustrative example, the method is described as it applies to vortex rings propagating up a tube. However, all parameters used are directly transferable to a development for vortex pairs in a channel (in fact, the mathematics is much simpler in this case). The basic approach taken here, that of using the bubble size and shape to generate the needed parameters which describe the potential field, should be applicable to other more complicated closed-vortex systems as well—for example, the helical vortex structure in the wake of helicopter rotors.

One way to find which groups of parameters are to be related is through dimensional analysis. Figure 2 shows the streamlines of a vortex ring fixed in space and in a frame attached to the moving vortex. In the fixed frame the streamlines have a dipolar character. When we transfer to a frame moving with the vortex ring, however, a region of irrotational fluid confined to move with the vortex core is identified. When the vortex ring is dyed on formation, the extent of this bubble region can be visualized as the vortex evolves.

Let us list in the moving frame of reference the parameters which would enter into a dimensional analysis. We designate as the dependent variable, U, the velocity of the vortex ring. The independent variables on which U must depend are: 1) the total circulation Γ; 2) the size of the vortex bubble which we designate by R^*, where R^* can be either R, R', or $\sqrt[3]{V}$ (see Fig. 2); 3) T, the thickness of the bubble which together with R^* defines the bubble shape; and 4) ρ_o, the radius of the tube (considering a vortex ring propagating axisymmetrically up a tube). We have made the assumption that the vorticity is sufficiently concentrated that the vortex core can be modeled as a filament for the purpose of calculating the shape and size of the bubble; therefore, the parameter a/R should not enter into the analysis. Furthermore, for the purpose of computing the shape of the bubble, we are assuming that the circulation in the wake is such a small fraction of the total circulation that it can be neglected. We find later that these are good approximations for typical vortex rings. Thus, we can write general functional relationships as

$$U = f(\Gamma, R^*, T, \rho_o) \tag{8}$$

An application of the (Buckingham) pi theorem yields the desired parametrical relationships for a vortex ring in a tube (or a vortex pair in a channel):

$$\frac{UR^*}{\Gamma} = f\left(\frac{T}{R^*}, \frac{R^*}{\rho_o}\right) \tag{9}$$

A more complicated vortex system must include additional parameters which describe the more complicated vortex structure, whereas for an unbounded vortex ring R^*/ρ_o would be absent. Equation (9) is a more precise statement of Eq. (7) for vortex rings and pairs.

We compute the relationships between the three nondimensional parameters UR^*/Γ, T/R^*, and R^*/ρ_o using the potential form of the Biot-Savart law given by Eq. (5). These relationships are purely kinematic and apply at every instant in time where the model is sufficiently accurate. From flow visualization experiments we measure T, R^*, and U as the

vortex evolves, and inserting this information into the kinematic relationships, we compute Γ as a function of time.

This then is the basic method as it applies to vortex rings, vortex pairs and, if generalized somewhat, to more complicated closed-vortex systems.

Application to Vortex Rings in a Tube

Kinematic Relationships

In order to calculate the kinematic relationships among the three nondimensional parameters given in Eq. (9), we model the vortex ring as a circular vortex filament of strength Γ and radius R in a tube of radius ρ_o. The mathematical details can be found in Ref. 5; only some results will be presented here.

We begin by defining a potential function as in Eq. (4), and a stream function from

$$u_\rho = \frac{1}{\rho}\frac{\partial \Psi}{\partial z} \qquad u_z = -\frac{1}{\rho}\frac{\partial \Psi}{\partial \rho} \tag{10}$$

where ρ and z are the radial and axial coordinates in a cylindrical coordinate system. In addition, these functions are divided into two parts: that for an unbounded vortex ring (subscript o) and that portion induced by the presence of the tube (sub i):

$$\Phi = \Phi_o + \Phi_i \qquad \Psi = \Psi_o + \Psi_i \tag{11}$$

Φ_i is found by solving Laplace's equation with the condition $\partial\Phi/\partial\rho = 0$ at $\rho = \rho_o$. The solutions for the unbounded[7] and bounded[5] vortex rings in a fixed frame of reference are given in terms of Bessel functions by:

$$\Phi_o(\rho,z) = -\frac{\Gamma R}{2}\int_0^\infty e^{-kz} J_o(k\rho) J_1(kR)\,dk$$

$$\Phi_i(\rho,z) = -\frac{\Gamma R}{\pi}\int_0^\infty \frac{K_1(k\rho_o)}{I_1(k\rho_o)} I_1(kR) I_o(k\rho)\sin(kz)\,dk$$

$$\Psi_o(\rho,z) = -\frac{\Gamma R}{2}\rho\int_0^\infty e^{-kz} J_1(k\rho) J_1(kR)\,dk$$

$$\Psi_i(\rho,z) = \frac{\Gamma R}{\pi}\rho\int_0^\infty \frac{K_1(k\rho_o)}{I_1(k\rho_o)} I_1(kR) I_1(k\rho)\cos(kz)\,dk \tag{12}$$

To compute the streamline and potential fields on a computer,‡ these expressions were expanded into series in terms of the small parameter $\epsilon = R/\rho_o$. The expansions for the unbounded ring require two harmonic series for the regions $\rho \lesseqgtr R$; however, only a single series, uniformly valid throughout the flowfield, is required for each of the induced quantities.

The streamlines and constant potential lines in the fixed frame of reference are shown for a bounded vortex ring in Fig. 3. Comparing with the streamline pattern for an unbounded vortex ring (Fig. 2), we see that, although the flow is still basically dipolar in character, there is generally more axial flow which results from the presence of the boundaries.

To compute the potential field in a frame moving with the vortex ring, we must specify the ring velocity in a convenient way. As a first step, the velocity U is split into two parts, one part for an unbounded vortex and the other representing the velocity induced by the presence of the tube. In addition, the velocities are nondimensionalized in a manner consistent with Eq. (9):

$$\hat{U} = \hat{U}_o - \hat{U}_i = \frac{U}{\Gamma/4\pi R} \tag{13}$$

‡Computations were performed on a PDP 11/45 computer.

So that the velocity can be conveniently varied, both $\hat{U}_o$ and $\hat{U}_i$ are parametrized in terms of variables with more physical relevance. $\hat{U}_i$ is expressed in terms of ϵ by evaluating $\partial\Phi_i/\partial z$ at $(\rho,z) = (R,0)$ which, by the Kelvin/Helmholtz theorem, is the change in ring velocity due to the presence of the tube. The effect of the tube is to decrease the velocity over the same vortex ring in an unbounded flow. $\hat{U}_o$ is parametrized with the core parameter a/R, using a modified form of the Kelvin/Lamb formula for a thin-core vortex ring[8]:

$$\hat{U}_i = 5.007\epsilon^3 + 2.829\epsilon^5 + 2.441\epsilon^7 + 2.296\epsilon^9 + \ldots \tag{14}$$

$$\hat{U}_o = \ell n(8R/a) - \tfrac{1}{3} \tag{15}$$

It should be noted, however, that for the purpose of calculating our kinematic relationships, a/R is used only as a convenient parameter to characterize $\hat{U}_o$, and its use here should not imply the acceptance of the Kelvin/Lamb formula as an accurate representation of the velocity of a real vortex ring. The streamlines and constant potential lines are shown in a moving frame of reference for a bounded vortex ring in Fig. 4. In this frame the bubble can be identified.

Having already specified the first of the three nondimensional parameters required to compute the kinematic relationships (namely, $\hat{U}$), we can obtain the other two parameters, T/R' and R'/ρ_o, from the potential and streamline fields in this moving frame. R' is used rather than

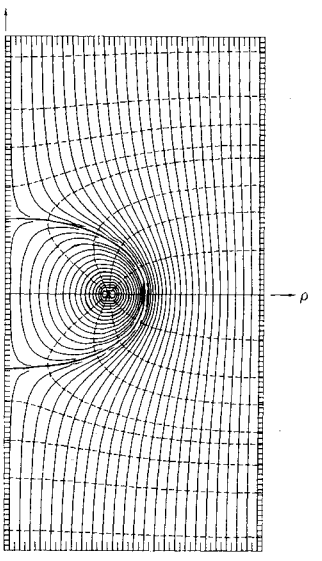

Fig. 4 Streamlines and lines of constant potential in the moving frame for a bounded vortex ring, $\epsilon = 0.40$, $a/R = 0.20$.

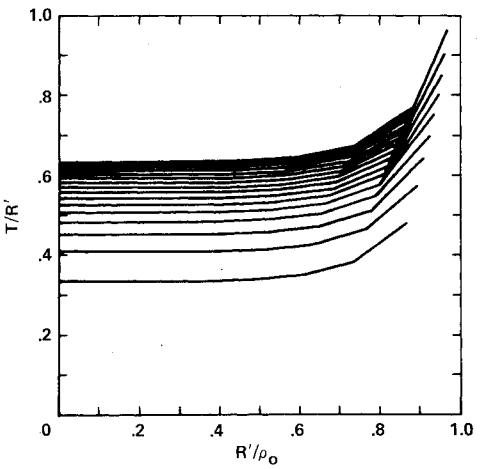

Fig. 5 Kinematic relationships for a vortex ring in a tube, beginning with the lowest curve $a/R = 0.04, 0.07, \ldots, 0.49$.

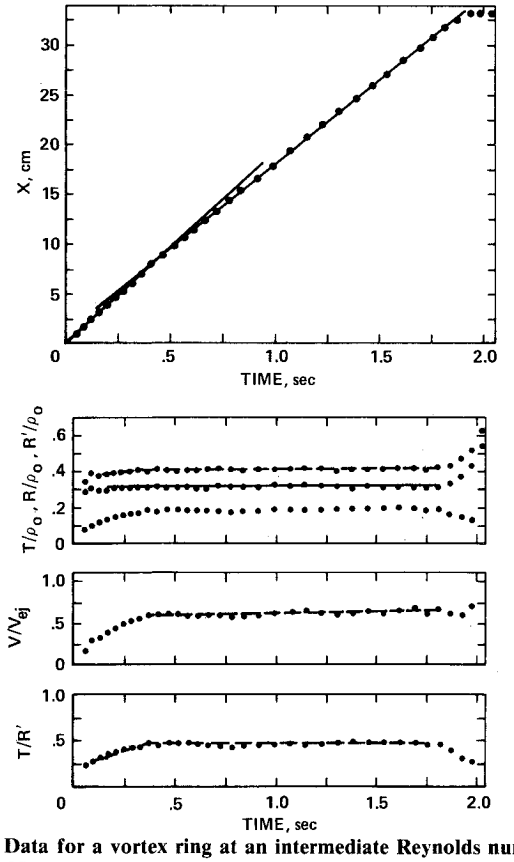

Fig. 6 Data for a vortex ring at an intermediate Reynolds number, $d/D = 0.25$, $Re_o = 7455$.

R because this quantity is more easily identified in flow visualization experiments. By systematically varying the values of a/R and ϵ, the kinematic relationships among the following parameters were calculated:

$$\frac{U}{\Gamma/4\pi R'}, \quad \frac{T}{R'}, \quad \text{and} \quad \frac{R'}{\rho_o} \tag{16}$$

These relationships are shown in Fig. 5 where T/R' is plotted against R'/ρ_o for different values of a/R. Note that vortex rings with either greater strength or lower velocity (keeping all other parameters constant) carry along with them greater amounts of irrotational fluid; the effect of the tube on this bubble region is to increase its volume further over an identical vortex ring in an unbounded flow.

The kinematic relationships expressed in Fig. 5 can be used in conjunction with flow visualization measurements to compute the total circulation of a vortex ring as it evolves. Such experiments will now be briefly described.

Flow Visualization Experiments

In a careful series of flow visualization experiments, vortex rings over a very wide range of Reynolds numbers were produced from a single ejection of water through orifices mounted in a tube. Seven different-sized orifices with orifice-to-tube diameters (d/D) from 0.10 to 0.64 were mounted in a plexiglass tube with a diameter of 11.88 cm and a length above the orifice of 40 cm. An hydraulically activated piston was used to eject a single pulse of water through the orifice over a period of about 0.170 s, producing a vortex ring which traveled up the tube. The piston speed was adjusted to yield three values of tube Reynolds numbers (based on piston speed and tube diameter) of roughly 5000, 4000, and 3000. In combination with the seven orifices, vortex rings were produced which varied in character from very viscous to highly turbulent over a Reynolds number range $Re \sim 690$-50,100, where $Re = 2RU/\nu$.

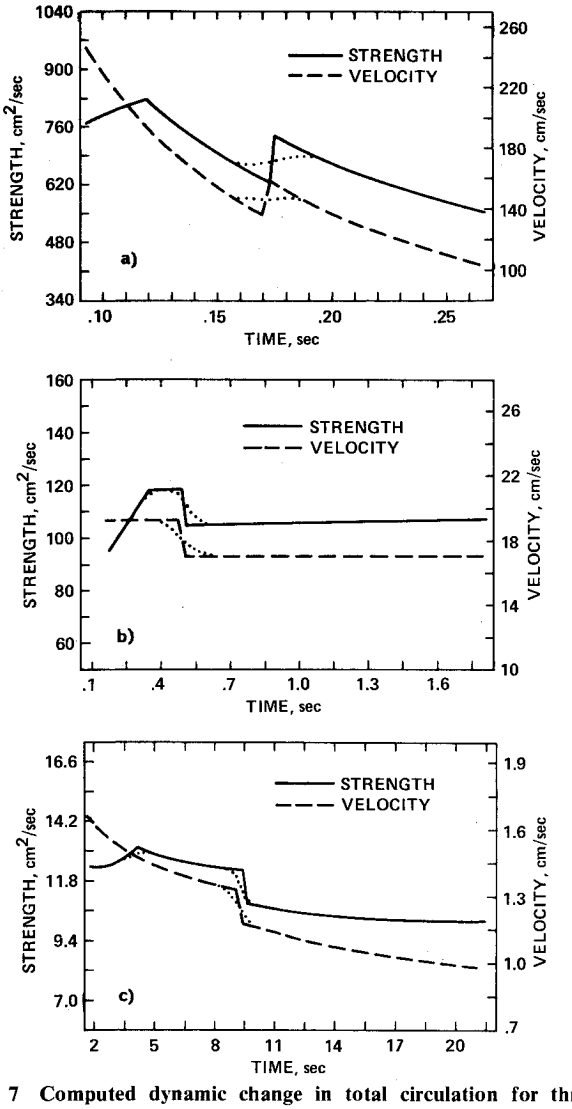

Fig. 7 Computed dynamic change in total circulation for three vortex rings: a) turbulent vortex ring, $Re_o = 50{,}144$, $d/D = 0.10$; b) "inviscid" vortex ring, $Re_o = 7455$, $d/D = 0.25$; and c) viscous vortex ring, $Re_o = 688$, $d/D = 0.64$.

To visualize the total extent of the vortex ring as it evolved, red food coloring was inserted into the chamber below the orifice. 16-mm movies at 100 frames/s were taken for all combinations of orifice size and tube Reynolds number. From these movies the following data were obtained for 17 cases at different Reynolds numbers: x, the distance from the orifice; R', the radius of the vortex ring to the edge of the dyed bubble; and T, the thickness of the dyed bubble. The measurements were made for individual vortex rings as they evolved, and all radial measurements were corrected for effects due to refraction of light.

A great deal of time and care was taken to obtain and refine the data. Since we are interested in the mean changes in strength resulting from the continuous diffusion of vorticity from the core, the values for $x(t)$ and $T/R'(t)$ were fit with piecewise-smooth curves. This was especially necessary for $x(t)$ since the velocity of the vortex ring was calculated from its derivative. An example of the data obtained for a vortex ring at an intermediate Reynolds number is shown in Fig. 6.

Combining the experimental data with the kinematic relationships of Fig. 5, the total circulation was calculated and plotted as a function of time for all 17 rings as they evolved. Results for three vortex rings at different Reynolds numbers are presented in Fig. 7. The strength of the vortex rings at the highest Reynolds numbers is found to decrease rapidly, consistent with rapid turbulent diffusion of vorticity from the core of the vortex. The rings at the lowest Reynolds numbers

are found to lose circulation at a much slower rate, consistent with the slow process of molecular diffusion. Over a wide range of intermediate Reynolds numbers, however, the vortex rings exhibit a basically inviscid character, with very little circulation being lost to a wake. At all Reynolds numbers, rapid changes in strength are found to occur periodically (due to fitting the data with piecewise-smooth curves, these appear as discontinuities in Γ and U), which are believed to result from the growth of unstable waves along the core and the periodic reorganization of the vortex core as these waves break. If found to exist in more general vortical flows, such behavior might play a role in the production of smaller scales of turbulence from the breakdown of larger eddies.

Accuracy of the Method

In developing the model from which the kinematic relationships between the total circulation and parameters describing the size and shape of the bubble were computed, we made two idealizations: 1) the vorticity is sufficiently concentrated that the finite extent of the core can be neglected, and 2) the circulation in the wake is such a small fraction of the total circulation it can be ignored.

To test the first hypothesis, 37 vortex filaments were distributed over the core of a vortex ring with core parameter $a/R = 0.25$, the average computed value for our experimentally produced vortex rings. The filaments were distributed over a roughly circular area and weighted according to the vorticity distribution in a real vortex ring as measured by Maxworthy.[2] Since the strongest vorticity sources are in the central portion of the core where streamlines are nearly circular, differences due to noncircular core shapes should be minor. Using the linearity property of the Biot-Savart law, the potential field was computed by summing the fields of the individual vortex filaments. Figure 8 compares the result with that for a single vortex filament having the same total circulation. Differences between the two are extremely small, there being virtually no difference in the values for T and R'.

To test the second hypothesis vorticity was distributed over 26 filaments in two rows in the wake region of the vortex ring. The filaments were weighted according to the calculated dynamic loss of total circulation from our experimental vortex ring at the highest Reynolds number (Fig. 7a), presumably the worst case. The stream-function fields computed for each filament were again summed; the result is shown in Fig. 9. The effect of the wake is to draw out the rear of the bubble somewhat, increasing the value of T. However, the difference in thickness is found to be only 3%, well within the precision of the experimental measurements.

The results of these two numerical experiments suggest that a vortex filament model is satisfactory for computing the size and shape of the vortex bubble. We would expect, however, that inaccuracies due to finite, noncircular cores, and wake vorticity will become significant at very low Reynolds numbers when vorticity is diffused over a large volume and not highly peaked.

To fully assess the accuracy of the method, direct comparisons should be made with independent calculations of total circulation. Ideally, one would like to obtain LDV measurements of the velocity along the axis of a vortex ring simultaneously with flow visualization measurements so that the integral of velocity around the core can be compared with the value of total circulation computed using the kinematic relationships of Fig. 5. Of three LDV measurements reported in the literature, one such comparison was possible using the results of Sullivan et al.[3] for a vortex ring in air at $Re = 3040$. A photograph from which the ratios T/R' and R'/R could be obtained was included for this case along with LDV measurements of U and R. Inserting these data into the kinematic relationships, the total circulation computed was found to be within 1% of the value reported in the article (see Fig. 10).

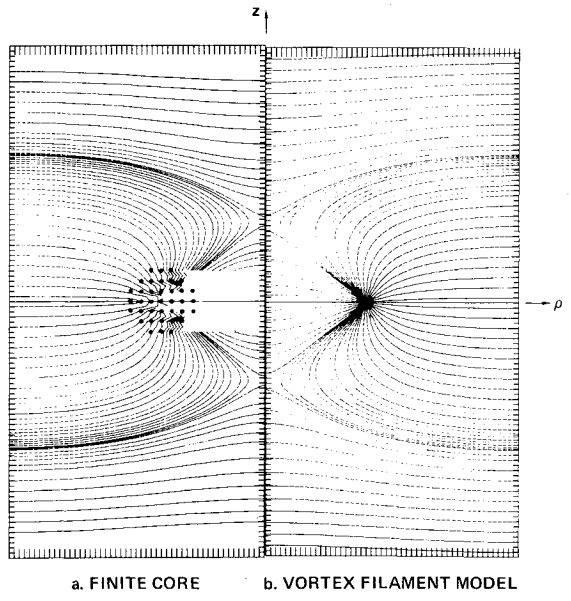

Fig. 8 Potential field comparison between a vortex ring with finite core and a single vortex filament, $\epsilon = 0.40$, $a/R = 0.25$.

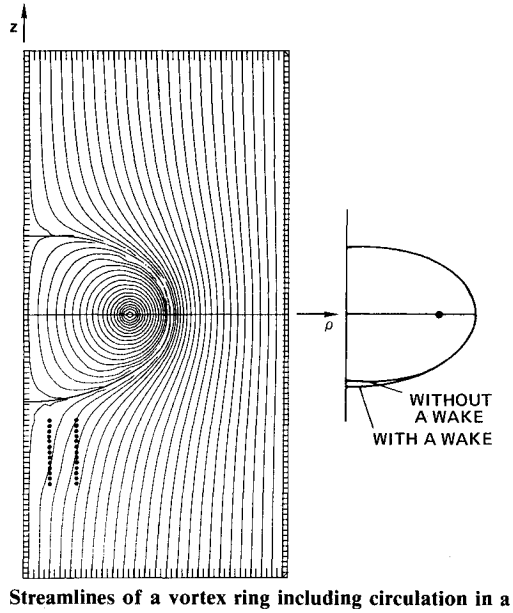

Fig. 9 Streamlines of a vortex ring including circulation in a wake, $\epsilon = 0.40$, $a/R = 0.25$.

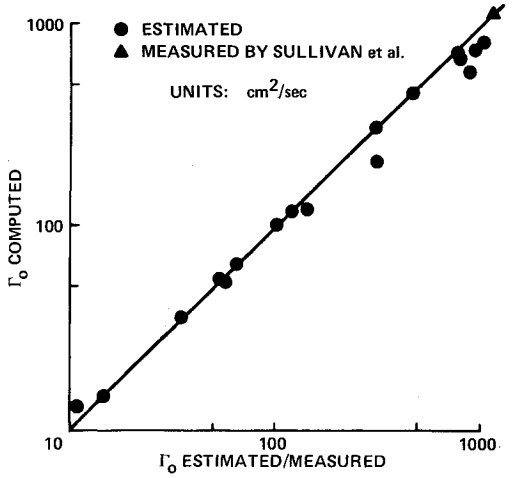

Fig. 10 Comparisons of total circulation computed using the kinematic relationships with estimates and an LDV measurement.

A different but less accurate comparison can also be made by estimating in an independent way the initial strengths of our experimental vortex rings. Consider a slug of fluid of length L ejected from the orifice with velocity $u_j(z)$; the total circulation content of this ejected fluid is given by

$$\Gamma_{ej} = \int_0^L u_j(z)\,dz \tag{17}$$

Measuring the initial volume of the vortex bubble, the total circulation in a newly formed vortex ring (defined as the point where Γ peaks) can be estimated by multiplying Γ_{ej} by the ratio of bubble volume to the total volume of fluid ejected from the orifice. The comparisons with these estimated values are shown in Fig. 10 and are felt to be quite good, especially considering the crudity of the estimates for Γ_o.

One additional comparison is possible. In the computation of the kinematic relationships, either R or R' could be used. Thus, in the course of computing Γ from U, T, and R', it is also possible to compute R. This calculation was performed for two vortex rings where an accurate flow visualization measurement of both R' and R was possible. A comparison of the measured values of R with the values computed using the fitted R' data is shown for the case in Fig. 6 (the solid line). In both cases the comparisons are excellent.

To fully assess the limits of accuracy of this method over a wide range of Reynolds numbers, additional LDV comparisons would be of interest. These tests, however, suggest that the strength of typical vortex rings can be accurately calculated from flow visualization measurements by making use of kinematic relationships which exist at all times between the vorticity and the velocity fields. Using this approach, calculations of dynamic changes in strength as a vortex evolves in time are now possible. Furthermore, a method for determining total circulation from flow visualization data should find a wide range of application in the study of flows in which are embedded regions of concentrated vorticity.

Acknowledgments

This work has been supported by the National Science Foundation under Grant No. ENG 74-22615, the Department of Aeronautics and Astronautics, and the Joint Institute for Aeronautics and Acoustics at Stanford University. The computer facility was made available by John Wilcox of the Institute for Plasma Research at Stanford.

References

[1] Riley, N., "Flows with Concentrated Vorticity: A Report on EUROMECH 41," *Journal of Fluid Mechanics,* Vol. 62, 1974, pp. 33-39.

[2] Maxworthy, T., "Some Experimental Studies of Vortex Rings," *Journal of Fluid Mechanics,* Vol. 81, 1977, pp. 465-495.

[3] Sullivan, J. P., Widnall, S. E., and Ezekiel, S., "Study of Vortex Rings using a Laser Doppler Velocimeter," *AIAA Journal,* Vol. 11, Oct. 1973, pp. 1384-1389.

[4] Sallet, D. W. and Widmayer, R. S., "An Experimental Investigation of Laminar and Turbulent Vortex Rings in Air," *Zeitschrift für Flugwissenschaften*, Band 22, 1974, pp. 207-215.

[5] Brasseur, J. G., "Kinematics and Dynamics of Vortex Rings in a Tube," Ph.D. Thesis, Stanford University, 1979.

[6] Batchelor, G. K., *An Introduction to Fluid Dynamics,* Cambridge University Press, England, 1965.

[7] Lamb, H., *Hydrodynamics,* Dover, New York, 1945, p. 239.

[8] Saffman, P. G., "The Velocity of Viscous Vortex Rings," *Studies in Applied Mathematics,* Vol. 49, 1970, pp. 371-380.